Journal of Biotechnology 152 (2011) 132–143

Contents lists available at ScienceDirect

Journal of Biotechnology

journal homepage: www.elsevier.com/locate/jbiotec

Amino acid uptake profiling of wild type and recombinant *Streptomyces lividans* TK24 batch fermentations

Pieter-Jan D'Huys[a], Ivan Lule[a], Sven Van Hove[a], Dominique Vercammen[a], Christine Wouters[b], Kristel Bernaerts[a], Jozef Anné[c], Jan F.M. Van Impe[a,*]

[a] *Chemical and Biochemical Process Technology and Control Section (BioTeC), Department of Chemical Engineering, Katholieke Universiteit Leuven, Willem de Croylaan 46, B-3001 Leuven, Belgium*
[b] *Laboratory of Applied Physical Chemistry and Environmental Technology, Department of Chemical Engineering, Katholieke Universiteit Leuven, Willem de Croylaan 46, B-3001 Leuven, Belgium*
[c] *Bacteriology Section, Department of Microbiology and Immunology, Katholieke Universiteit Leuven, Minderbroederstraat 10, 3000 Leuven, Belgium*

ARTICLE INFO

Article history:
Received 3 May 2010
Received in revised form 12 August 2010
Accepted 17 August 2010
Available online 24 August 2010

Keywords:
Streptomyces lividans
Heterologous protein production
Amino acid utilization
Metabolic footprint

ABSTRACT

Streptomyces lividans is considered an interesting host for the secretory production of heterologous proteins. To obtain a good secretion yield of heterologous proteins, the availability of suitable nitrogen sources in the medium is required. Often, undefined mixtures of amino acids are used to improve protein yields. However, the understanding of amino acid utilization as well as their contribution to the heterologous protein synthesis is poor.

In this paper, amino acid utilization by wild type and recombinant *S. lividans* TK24 growing on a minimal medium supplemented with casamino acids is profiled by intensive analysis of the exometabolome (metabolic footprint) as a function of time. Dynamics of biomass, substrates, by-products and heterologous protein are characterized, analyzed and compared. As an exemplary protein mouse Tumor Necrosis Factor Alpha (mTNF-α) is considered.

Results unveil preferential glutamate and aspartate assimilation, together with glucose and ammonium, but the associated high biomass growth rate is unfavorable for protein production. Excretion of organic acids as well as alanine is observed. Pyruvate and alanine overflow point at an imbalance between carbon and nitrogen catabolism and biosynthetic fluxes. Lactate secretion is probably related to clump formation. Heterologous protein production induces a slowdown in growth, denser clump formation and a shift in metabolism, as reflected in the altered substrate requirements and overflow pattern. Besides glutamate and aspartate, most amino acids are catabolized, however, their exact contribution in heterologous protein production could not be seized from macroscopic quantities.

The metabolic footprints presented in this paper provide a first insight into the impact and relevance of amino acids on biomass growth and protein production. Type and availability of substrates together with biomass growth rate and morphology affect the protein secretion efficiency and should be optimally controlled, e.g., by appropriate medium formulation and substrate dosing. Overflow metabolism as well as high biomass growth rates must be avoided because they reduce protein yields. Further investigation of the intracellular metabolic fluxes should be conducted to fully unravel and identify ways to relieve the metabolic burden of plasmid maintenance and heterologous protein production and to prevent overflow.

1. Introduction

Streptomycetes are filamentous Gram-positive soil-dwelling bacteria with a complex morphological and physiological life cycle. Their metabolism and its regulation is strongly related to this soil environment which is carbon-rich but nitrogen- and phosphate-poor (Hodgson, 2000). *Streptomycetes* are industrially important because of their capacity to synthesize and secrete a wide range of secondary metabolites, particularly antibiotics, which are extensively used in agricultural, environmental and pharmaceu-

Abbreviations: mTNF-α, mouse Tumor Necrosis Factor alpha; WT, *S. lividans* strain TK24; PL, *S. lividans* strain TK24 harboring empty pIJ486 plasmid; REC, *S. lividans* strain TK24 harboring *mTNF-α* gene on pIJ486 plasmid; GP, growth phase; GABA, gamma-aminobutyric acid.

* Corresponding author. Tel.: +32 16 32 14 66; fax: +32 16 32 29 91.
E-mail addresses: kristel.bernaerts@cit.kuleuven.be (K. Bernaerts), jozef.anne@rega.kuleuven.be (J. Anné), jan.vanimpe@cit.kuleuven.be (J.F.M. Van Impe).

0168-1656/$ – see front matter © 2010 Elsevier B.V. All rights reserved.
doi:10.1016/j.jbiotec.2010.08.011

tical industry (e.g., Gilbert et al., 1995). Besides the relevance of their natural products, *Streptomycetes* are considered as interesting hosts for heterologous protein production (e.g., Binnie et al., 1997; Nakashima et al., 2005; Vrancken and Anné, 2009). In most cases, heterologous genes are linked to signal peptides of strongly expressed/secreted endogenous *Streptomyces* proteins. Signal peptides act as address tags specifically recognizing the Sec-translocase which is positioned at the cell membrane (Economou, 1999; van Wely et al., 2001). Within the Sec-dependent secretion system, SecA (a precursor protein stimulated ATPase) takes a central role being the molecular motor driving translocation (van Wely et al., 2001). Besides Sec-dependent secretion, Tat-dependent secretion is also active in, e.g., *S. lividans* (Schaerlaekens et al., 2004) but is not always as efficient.

Particularly, *Streptomyces lividans* holds great potential as a high-valued industrial host cell in heterologous protein production (such as biopharmaceuticals and enzymes). *S. lividans* can (i) secrete biologically active proteins (of either bacterial or eurkaryotic origin) in relatively high amounts which are easily recoverable from fermentation media, (ii) exhibits a limited protease activity, and (iii) is biologically safe (e.g., Van Mellaert and Anné, 1999; Vrancken and Anné, 2009). Examples in which *S. lividans* is exploited as a secretion platform for therapeutic proteins or industrial enzymes are reported in, e.g., Van Mellaert and Anné (1999), Pozidis et al. (2001), Sianidis et al. (2006), Ayadi et al. (2007) and Pimienta et al. (2007).

Media for heterologous protein production in *Streptomyces* strains, and also for other micro-organisms, are typically rich media containing sufficient amounts of amino acids (e.g., Pozidis et al., 2001; Görgens et al., 2005a,b). Transport mechanisms for amino acids in *Streptomycetes* are reviewed in Hodgson (2000). For *Streptomyces*, five types of permeases have been identified: a neutral amino acid permease, an energy-dependent arginine specific permease, an energy-dependent basic permease, an energy-dependent acidic amino acid permease and a constitutive proline-specific transporter. Usage of amino acids can occur in a preferential manner with respect to other amino acids and/or carbon sources. For example, as found by Corvini et al. (2004), *S. pristinaespiralis* will start using glutamate, then arginine together with glucose (in a synthetic medium containing these components and no other N-sources). In other cases, co-metabolism of a number of amino acids with a carbon source, such as glucose, is reported (Voelker and Altaba, 2001; Bapat et al., 2006). However, in general, the amino acid uptake mechanisms and catabolism are poorly understood for *Streptomycetes*. Furthermore, many studies report observations for different *Streptomyces* species.

In view of optimization of production levels of heterologous proteins in *S. lividans*, a better understanding of the effects of C- and N-substrates on the metabolism and protein production capacity of the cell is necessary. A first step in this direction has been taken by Nowruzi et al. (2008), whom report a systematic approach to identify and optimize the essential amino acids in defined minimal medium for human interleukin 3 production by *S. lividans* 66. However, based on this screening approach, no information is gained on the uptake mechanism nor the utilization dynamics of amino acids and their role or significance in growth and/or heterologous protein formation. Recently, Kassama et al. (2010) reported the metabolic fingerprint for mTNF-α secreting *S. lividans* TK24 (grown in phage medium) in comparison with the metabolic fingerprint of the non-secreting wild type and a wild type carrying the empty plasmid. Multi-block principal component analysis revealed that many intracellular metabolite levels (e.g., alanine, leucine, succinate) are at least tenfold higher in *S. lividans* expressing mTNF-α or containing empty plasmid as compared to the wild type. This observation is a reflection of the metabolic burden of heterologous protein biosynthesis and plasmid maintenance. This metabolic burden is caused by the competition for host cell's resources, such as energy-containing components (ATP), precursor metabolites and reductive power (NADPH) (see, e.g., Glick, 1995).

In view of further unraveling the response of the host cell's metabolism to heterologous protein production by *S. lividans*, this paper characterizes growth, substrate utilization, by-product formation and protein production in the presence of a complex mixture of amino acids, namely casamino acids. *S. lividans* TK24 producing mouse Tumor Necrosis Factor alpha (mTNF-α), as a relevant example protein, is compared with the non-secreting wild type and plasmid-containing strain. Furthermore, this metabolic profiling of the extracellular environment allows the analysis of specific requirements (in terms of yields and specific conversion rates) of the protein secreting strain.

2. Material and methods

2.1. Bacterial strains

Streptomyces lividans TK24 was kindly provided by the John Innes Centre, Norwich, UK. Three strains are used in this study: (i) *S. lividans* TK24, denoted as wild type (WT), (ii) recombinant *S. lividans* TK24 harboring empty pIJ486 plasmid, denoted as plasmid-containing strain (PL), and (iii) recombinant *S. lividans* TK24 secreting mTNF-α, denoted as protein-producing strain (REC). The mTNF-α secreting *S. lividans* strains contains pIJ486 plasmid in which mTNFα-cDNA is cloned behind a strong promoter and signal peptide sequence of *Streptomyces venezuelae* subtilisin inhibitor gene (*vsi*) (Pozidis et al., 2001, Lammertyn et al., 1997). All DNA manipulations were done as described by Kieser et al. (2000).

The stock culture was maintained as a homogenized mycelium suspension at −80 °C in 20% v/v glycerol. The mycelium suspension was made by homogenizing a cell suspension grown in phage medium (Korn et al., 1978) (10 g/L glucose, 5 g/L tryptone, 5 g/L yeast extract, 5 g/L LabM, 0.74 g/L $CaCl_2{\cdot}2H_2O$, 0.5 g/L $MgSO_4{\cdot}7H_2O$, and pH 7.2) for 48 h at 28 °C and 250 rpm. Growth of the recombinant strains was in the presence of thiostrepton (50 μg/mL) to select for plasmid maintenance.

2.2. Bioreactor experiments

Batch experiments were performed in a bench-top 5-Litre BioFlo 3000 bioreactor (New Brunswick Scientific). The reactor was filled with 3 L culture medium. Temperature was set at 30 °C, the rotation speed and aeration flow were fixed at 400 rpm and 2 L/min. pH was kept constant at 7 by automated addition of 1N H_2SO_4 and 1N NaOH. Dissolved oxygen was not controlled but was never depleted during the experiments.

Pre-cultures were grown for 48 h in 5 mL phage medium at 30 °C and 250 rpm (see Section 2.1). This pre-culture was homogenized and transferred in a volume ratio of 1/50 in a shake-flask containing 50 mL phage medium (containing 50 μg/mL thiostrepton), which was subsequently incubated for 48 h at 30 °C and 250 rpm.

Cells from four flasks were harvested by centrifugation (10 min at 3200 × *g*) and removing the spent medium. The pellets were re-dissolved in a small aliquot of reactor medium, i.e., slightly modified minimal liquid medium (NMMP): 10 g/L glucose, 3 g/L $(NH_4)_2SO_4$, 5 g/L or 15 g/L Bacto™ casamino acids, 0.6 g/L $MgSO_4{\cdot}7H_2O$, 2.7 g/L NaH_2PO_4, 3.92 g/L K_2HPO_4 and 1 mL/L minor elements solution (containing 1 g/L $ZnSO_4{\cdot}7H_2O$, 1 g/L $FeSO_4{\cdot}7H_2O$, 1 g/L $MnCl_2{\cdot}4H_2O$ and 1 g/L anhydrous $CaCl_2$) (Kieser et al., 2000). The casamino acids content was varied (5 or 15 g/L) and the ammonium content (from $(NH_4)_2SO_4$) was increased (1.5×) to make sure that NH_4^+ was not growth-limiting. Antifoam (antifoam Y-30 emulsion, Sigma) was added at the start and at regular time intervals to avoid extensive foam formation.

2.3. Analytical procedures

2.3.1. Biomass

Biomass was measured as cell dry weight (DW) by filtering 5 mL of the culture filtered through a predried filter (Supor®-200 0.2 μm mm membrane filter. Pall Corporation, Michigan, USA) and drying to constant weight at 105 °C for 24 h. The filtrate was kept for analysis of the extracellular metabolites. Data shown are the average of triplicate measurements.

2.3.2. Test kits

Glucose was determined by means of the glucose dehydrogenase test (Gluc-DH, Ecoline® S+, Diagnostic Systems). Ammonium was determined with the ammonia testkit of Boehringer Mannheim/R-biopharm. Spectrophotometric measurements were done with the Genesys 10S spectrophotometer (Thermo Spectronic). Phospate (PO_4^{3-}) was quantified spectrophotometrically (DR 5000, Hach-Lange GMBH) by means of the phosphate detection kit LCK 350 (Hach-Lange GMBH). Measurement errors were approximately 5–10%.

2.3.3. Organic acids measurements

Pyruvic acid, lactic acid, α-ketoglutaric acid and succinic acid concentrations were determined by gas chromatography (Finnigan Trace GC Ultra) with a Stabilwax®-DA column (30 m × 0.32 mmID) and a flame ionization detector. External standards were used for calibration procedures. A volume of 1.9 mL of external standard or filtrate for organic acid measurement was prepared for gas chromatography by adding 100 μL isobutyric acid as an internal standard and subsequent methylation (Drummond and Shama, 1982). Measurement errors were approximately 5–10%.

2.3.4. Amino acids measurements

Amino acids were measured using the EZ:faast™ GC–MS amino acid analysis kit of Phenomenex. Using a Perkin Elmer Autosystem XL-Turbomass Gold GC–MS and norvaline as internal standard, this method was able to analyze the samples for all amino acids present in the casamino acids mixture, except for arginine and cysteine. The Perkin Elmer Autosystem XL gas chromatograph was directly coupled to a Perkin Elmer Turbomass Gold mass spectrometer. The Zebron ZB-AAA capillary column supplied with the test kit and a Siltek deactivated split/splitless liner was used. The carrier gas (He) flow was kept constant at 1.1 mL/min. The oven temperature program was as follows: initial temperature 110 °C for 1 min, a 30 °C/min ramp to 320 °C, held for 1 min. The temperature of the injection port was 275 °C. The MS temperatures were as follows: inlet line temperature 320 °C and ion source 240 °C. The scan range was 50–350 (12.5 scans/s). Under these conditions a 2 μL sample was injected with a capillary PSS injector in split (10 mL/min) mode. Calibration curves were prepared according to the manufactures instruction for a range of 20–400 μmol/L. Samples were analyzed in triplicate. Fig. 1 shows a typical chromatogram measured for casamino acids in Bacto™ casamino acids technical.

2.3.5. Protein measurements

mTNF-α was measured using the mTNF-α ELISA kit from Diamed Eurogen. A standard curve was set up by plotting the absorbance of each standard versus the corresponding protein concentration. The unknown mTNF-α concentrations in the samples were subsequently derived from the established standard curve.

2.4. Data analysis

All data analysis was performed in Matlab R2006a (Version 7.2., Mathworks, MA, USA).

2.4.1. Data alignment

Biomass data were fitted with a multi-phase linear model in order to identify different phases, i.e., the lag phase, (possibly) multiple exponential growth phases and the stationary phase. The death phase is not considered. If needed, a transition phase (without growth) between the exponential growth phases was allowed. Parameters were obtained by fitting ln(DW)-data using the optimization routine *fmincon*. The statistical significance of the multiple exponential phases was verified. Data from various experiments were subsequently aligned with respect to the end point of the lag phase. Biomass data are aligned along both the time and ln(DW)-axis. Full details are given in Supplement 1.

2.4.2. Yield calculations

Yield coefficients with respect to biomass were derived by plotting amino acid concentrations as a function of corresponding biomass concentration and performing a linear regression in each growth phase (considering only the data exhibiting a constant stoichiometry). Based on the estimated yield values and the specific growth rate derived from the multi-phase linear model, the specific consumption/production rates were calculated.

3. Results

Experimental data are summarized in a number of overview graphs, i.e., Figs. 2, 3, 5 and 6. Complementary, the yield coefficients and specific conversion rates are calculated and plotted in Fig. 4. These results are systematically introduced in the following sections. After presenting the outcome of the data alignment procedure and the identification of (growth) phases (Section 3.1) and discussing the composition of Bacto™ casamino acids (Section 3.2), the metabolic footprint (or exometabolome) for *S. lividans* TK24 (WT) strain grown in NMMP with 5 g/L casamino acids is given (Section 3.3). Next, the effect of an increase of the amino acid content on the physiology of the WT strain is presented (Section 3.4). The last Section 3.5 presents the metabolic footprints for the plasmid-containing strain (PL) and the mTNF-α producing strain (REC).

3.1. Data pre-processing

Variability in the inoculum size and, more importantly, in the duration of the lag phase, hampers easy comparison of concentration profiles from different experiments. To overcome this hurdle, a data pre-processing step is performed in which all data are aligned by lining up the lag (or adaptation) phase observed in the biomass dry weight data (see Section 2.4). Time is re-scaled by subtracting the lag phase duration from the actual elapsed fermentation time. Biomass data are also aligned to equalize initial biomass values. The methodology is illustrated in Supplement 1. The multi-phase linear model applied for data alignment also allows identification of the presence of multiple exponential growth phases. An overview of the model parameters characterizing the biomass data is given in Table 1. The different growth phases are demarked by horizontal lines in the figures with concentration data.

3.2. Composition of Bacto™ casamino acids

Casamino acids contains all essential amino acids except tryptophan, glutamine and asparagine. The composition of casamino acids varies amongst different batches (due to product variability). Although the exact amounts may differ, Table 2 gives a good representation of the average casamino acids composition. Glutamate, aspartate, leucine and proline are most abundant.

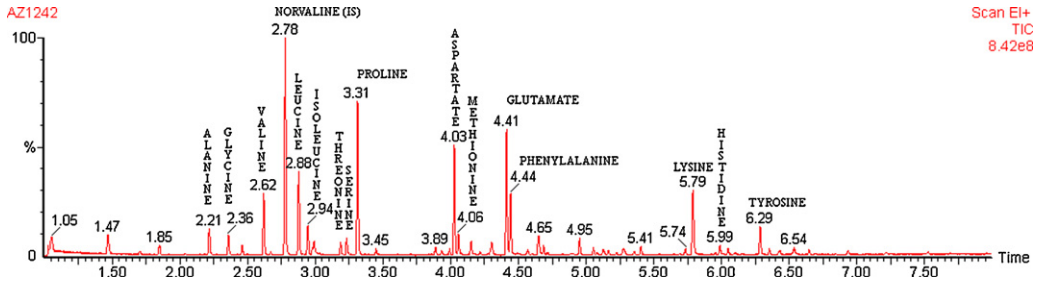

Fig. 1. Example of a chromatogram of the amino acids analysis in Bacto™ casamino acids technical analyzed with the EZ:faast™ kit for GC–MS (Phenomenex). Elution order and time (min): alanine (2.21), glycine (2.36), valine (2.62), norvaline IS (2.78), leucine (2.88), isoleucine (2.94), threonine (3.19), serine (3.23), proline (3.31), aspartate (4.03), methionine (4.06), glutamate (4.41), phenylalanine (4.44), lysine (5.79), histidine (5.99), tyrosine (6.29).

Table 1
Lag and growth parameters obtained by fitting a multi-phase linear model on ln(DW)-data, with λ the lag phase duration, and μ_i the specific growth rate of the ith growth phase. Standard deviations are given between brackets.

	WT 5 g/L CAS	WT 15 g/L CAS	PL 5 g/L CAS	REC 5 g/L CAS [a]
λ (h)	8.689 (2.182×10^{-1})	12.041 (2.357×10^{-2})	6.231 (8.948×10^{-2})	6.466 (7.003×10^{-1})
μ_1 (h^{-1})	1.401×10^{-1} (3.836×10^{-3})	1.129×10^{-1} (2.169×10^{-4})	9.901×10^{-2} (5.028×10^{-3})	7.630×10^{-2} (1.821×10^{-3})
μ_2 (h^{-1})	6.328×10^{-2} (4.111×10^{-3})	n.d.	3.439×10^{-2} (1.762×10^{-3})	3.607×10^{-2} (4.841×10^{-3})

n.d.: not detected.
[a] A transition period without growth is estimated between the two exponential growth phases.

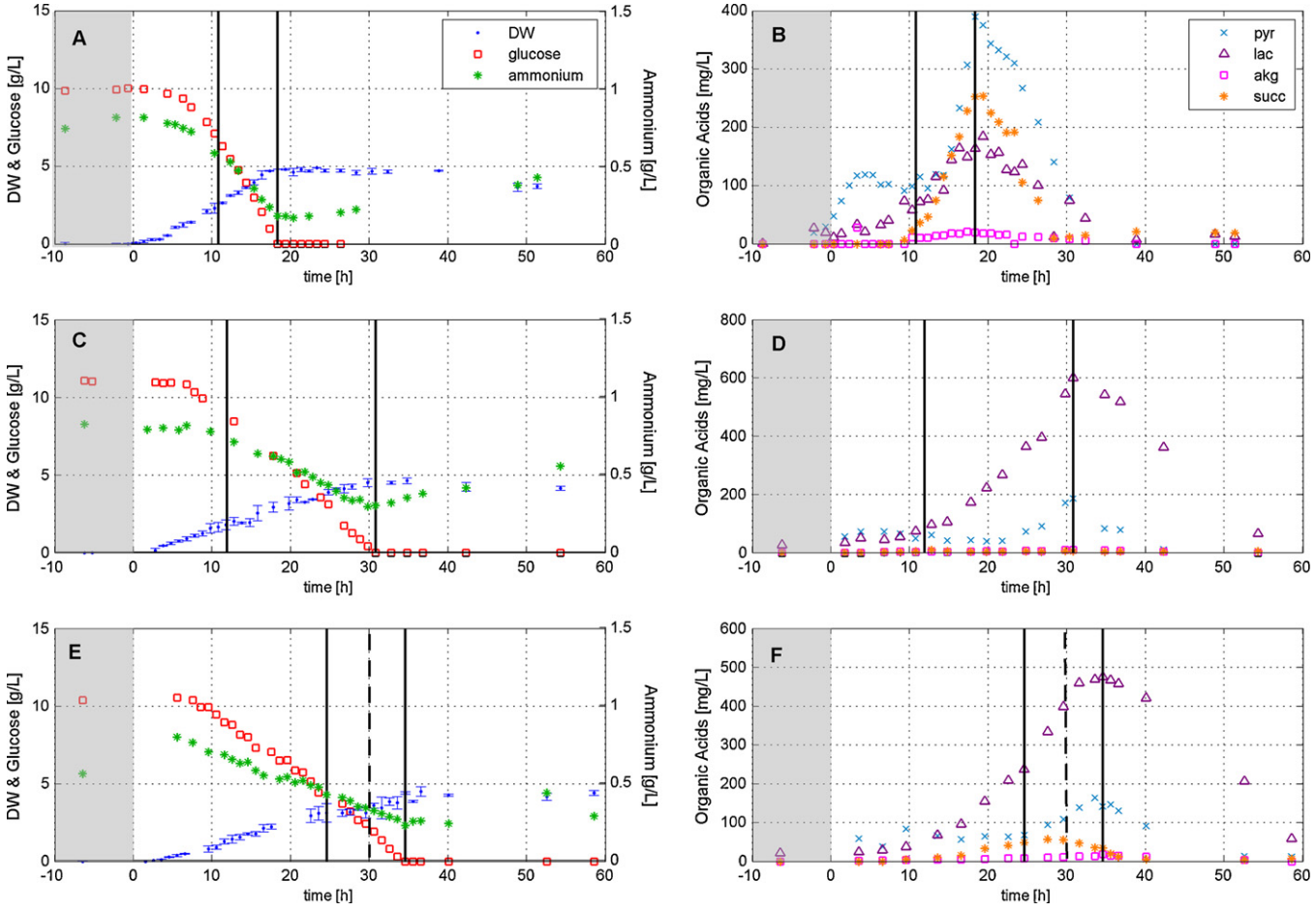

Fig. 2. Experimental data for *S. lividans* TK24 wild type (WT) (A and B), plasmid-containing (PL) (C and D) and protein-producing (REC) (E and F) strain, respectively, grown on NMMP containing 5 g/L casmino acids. Left plots: biomass (●), glucose (□), ammonium (✱). Right plots: lactate (△), pyruvate (×), α-ketoglutarate (□), succinate (✱). Full vertical lines demarcate growth phases (reflected by glutamate and aspartate depletion (GP1) and glucose depletion (GP2)). The dashed vertical line demarcates the end of the adaptation period (without growth) between GP1 and GP2 for the REC strain.

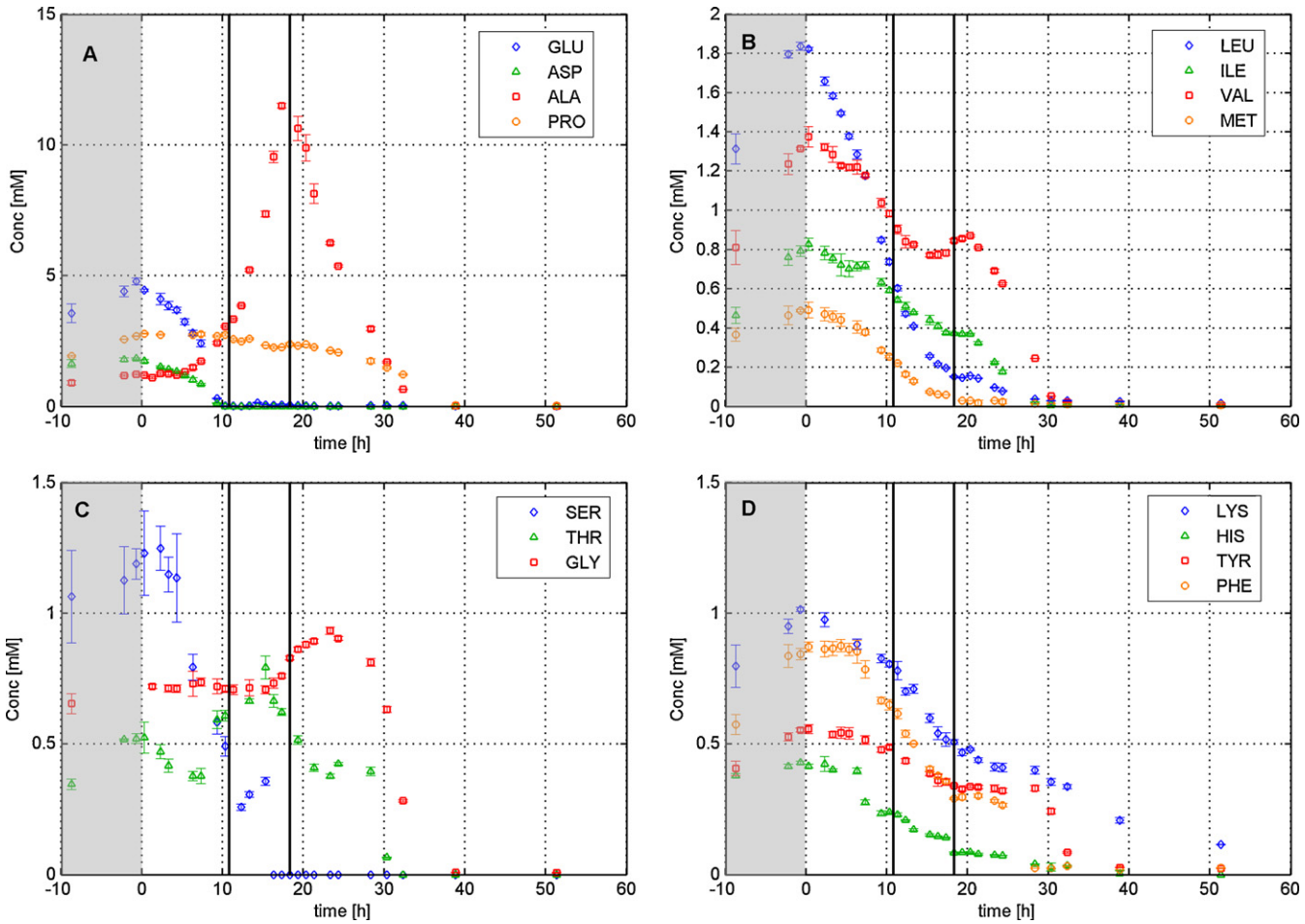

Fig. 3. Amino acid concentration data for *S. lividans* TK24 wild type strain (WT) grown on NMMP containing 5 g/L casmino acids. (A) Glutamate (GLU), aspartate (ASP), alanine (ALA) and proline (PRO). (B) Leucine (LEU), isoleucine (ILE), valine (VAL) and methionine (MET). (C) Serine (SER), threonine (THR) and glycine (GLY). (D) Lysine (LYS), histidine (HIS), tyrosine (TYR) and phenylalanine (PHE). Vertical lines demarcate growth phases (reflected by glutamate and aspartate depletion (GP1) and glucose depletion (GP2)).

3.3. *Metabolic footprint of S. lividans TK24 grown on NMMP with 5 g/L casamino acids*

Figs. 2 (top plots) and 3 summarize all concentration data: biomass, substrates and secreted by-products for *S. lividans* TK24 (denoted as WT) grown on NMMP with 5 g/L casamino acids. Yield coefficients, representing the amount of amino acid consumed/produced per gram of dry biomass weight formed, and accompanying specific uptake/production rates for substrates/products are summarized in Fig. 4. Exact values are provided in Supplement 2.

Biomass data, as depicted in Fig. 2A, exhibit an initial lag phase, two exponential growth phases with distinct specific growth rate (Table 1), and a stationary phase. The first exponential growth phase (GP1), with a specific growth rate of 0.14 h^{-1}, ends when glutamate and aspartate are depleted (see Figs. 2A and 3A). The specific growth rate then decreases to a substantially lower value of 0.063 h^{-1} (GP2) until glucose is exhausted. The specific growth rate of the first phase is dictated by the consumption of glutamate, aspartate, glucose and ammonium, while the specific growth rate in the second phase is particularly determined by the consumption of glucose and ammonium. Glutamate and aspartate clearly act as preferential substrates (both as C- and N-source) complementary to glucose and ammonium and augment the biomass formation rate in GP1. Phosphate is abundant throughout the whole experiment (final concentration ca. 1 g/L PO_4^{3-}) and thus not growth-limiting.

Several organic acids are produced (Fig. 2B). Pyruvic acid is most predominant followed by succinic acid, lactic acid and α-ketoglutaric acid. Pyruvate accumulates in both exponential phases. Succinic and α-ketoglutaric acid accumulate in the second growth phase. All organic acids are eventually reused during the stationary phase, i.e., when biomass accumulation ceases.

As shown in Fig. 3, significant changes in the concentrations of the 15 measured amino acids can be observed. During the lag phase, the amino acid levels tend to increase. Since Bacto™ casamino acids contains small amounts of peptides, this increase can likely be assigned to peptide breakdown. An alternative and maybe complementary explanation could be that cells acclimatize to the new environment by adjusting their intracellular pools of amino acids.

Table 2
Measured free amino acids (mg/g casamino acids) in Bacto™ casamino acids technical (data from WT 5 g/L CAS experiment). Arginine and cysteine cannot be measured (n.d.).

VAL	31.8	LEU	39.3
TYR	14.48	ILE	14.41
TRP	0	HIS	12.4
THR	10.7	GLY	12
SER	20	GLU	102.9
PRO	46	CYS	n.d.
PHE	19.8	ASP	42.56
MET	11.92	ARG	n.d.
LYS	23.36	ALA	17.8
GLN	0	ASN	0

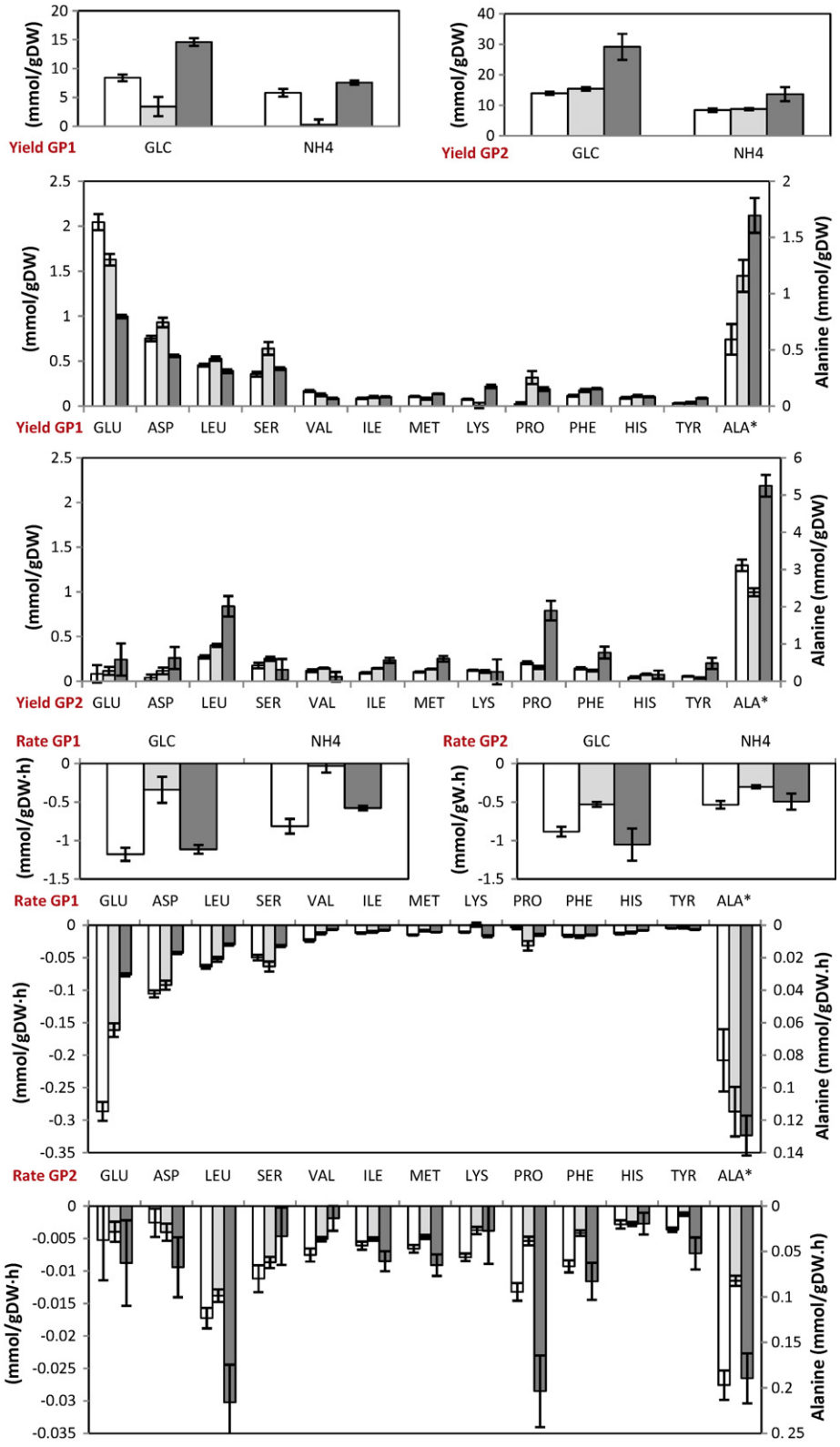

Fig. 4. Yield coefficients representing the amount of component (glucose, ammonium or amino acids) consumed/produced per gram of dry biomass weight formed during the exponential phases (above) and specific uptake/production rates (below) for *S. lividans* TK24 wild type (white bars), plasmid-containing (light grey bars) and protein-producing (dark grey bars) strain. Except for alanine, that is produced during the exponential phase, all components are to be considered as substrates (uptake).

However, such hypothesis can only be confirmed by measurement of intracellular pool sizes.

During the exponential growth phases, many amino acid concentration data exhibit an overall decreasing trend. The sequence of uptake is as follows: (i) uptake of glutamate, aspartate (Fig. 3A), serine (Fig. 3C), leucine, isoleucine, valine, methionine (Fig. 3B) and lysine (Fig. 3D) is initiated together with biomass growth, i.e., immediately after ending the lag phase, (ii) uptake of phenylala-

nine, tyrosine, histidine (Fig. 3D) and proline (Fig. 3A) is delayed, and (iii) alanine (Fig. 3A) and glycine (Fig. 3C) are taken up during the stationary phase. Threonine data are too fluctuating to decipher any trend (thus not taken up in Fig. 4 or Supplement 2).

Out of all amino acids, glutamate has by far the greatest uptake rate in GP1, followed by aspartate, leucine and serine (see specific rates in Fig. 4). The uptake rates of the other amino acids are up to ten times smaller. Proline is not consumed during the first phase. During the second growth phase, the specific uptake rates of proline and leucine are the largest. Comparing the yields in both growth phases (Fig. 4), glutamate followed by aspartate, leucine and serine, respectively, have the highest yield in GP1, while leucine and proline are most consumed per gram dry weight in GP2. Whereas the specific uptake rates of most amino acids are higher in GP1 as in GP2, this trend does not hold for amino acid yields (see ratios in Supplement 2).

Alanine and glycine are special cases in this study. They are not consumed during either growth phase, on the contrary a huge amount of alanine is secreted during both growth phases. The alanine concentration peaks just before initiation of the stationary phase. Alanine is produced in both growth phases, but with the highest specific production rate in the second growth phase (Fig. 4). To a much lesser extent as alanine, an increase in glycine is observed near the end of GP2.

Although growth ceases in the stationary phase, uptake of the remaining amino acids proceeds (with or without a delay in time). The surplus of ammonium generated by amino acids deamination is secreted (Fig. 2A). Alanine is also consumed. Glycine shows a further increase in the beginning of the stationary phase but is eventually also taken up (Fig. 2C). Except for lysine, all amino acids are finally depleted from the medium.

3.4. Metabolic footprint of S. lividans TK24 grown on NMMP with 15 g/L casamino acids

Fig. 5 displays the metabolic footprint of the WT strain when tripling the casamino acid content in the culture medium. On the whole, substrate profiles, including consumed amino acids, depict similar trends as for the WT grown in the presence of 5 g/L casamino acids. When entering GP1, an increase of valine, isoleucine, lysine, histidine, tyrosine and phenylalanine (see Fig. 5D and F) can be observed. Most likely, this increase can be explained by the liberation of free amino acids by breakdown of peptides in Bacto™ casamino acids. Any uptake of these amino acids is in that case camouflaged.

Glucose, ammonium, glutamate and aspartate are again co-metabolized as main substrates. Glutamate and aspartate are depleted almost simultaneously with glucose. Consequently, a single growth phase, characterized by a constant specific growth rate, is detected, with the end corresponding with the moment of glucose exhaustion (see Table 1 and Fig. 5A). Since the four main substrates, being glucose, ammonium, glutamate and aspartate, are non-limiting during the whole growth phase, there is only one exponential growth phase and a comparable specific biomass growth rate as for GP1 in NMMP with 5 g/L casamino acids would be expected. However, as shown in Table 1, the specific growth rate is lower. This observation could point at an inhibitory effect of one or more amino acids at this higher concentration. The specific uptake rates of glutamate and aspartate are indeed lower for this experiment (i.e., 2.86×10^{-1} decreased to 2.55×10^{-1} mmol/gDW h for glutamate, and 1.06×10^{-1} decreased to 6.82×10^{-2} mmol/gDW h for aspartate). On the other hand, a substantial part of the amino acids is build into biomass since the total amount of biomass increased.

Ammonium data exhibit a rise in concentration at the start of the experiment. This liberation of ammonium may be due to many processes, but is likely to be correlated with ammonium liberation upon catabolic breakdown of consumed amino acids.

Looking at the organic acid profiles, succinate excretion has drastically increased as compared to the WT experiment on 5 g/L casamino acids and succinate is now predominant besides pyruvate. Pyruvate peaks again at the moment of glucose depletion and the total amount of pyruvate is comparable with that in the WT experiment on 5 g/L casamino acids. The lactate and α-ketoglutarate concentration profiles and levels are also very similar with the WT experiment on 5 g/L casamino acids. To conclude, alanine is again abundantly secreted (up to 2.23 g/L), approximately twice as much as with 5 g/L casamino acids.

3.5. Metabolic footprints for plasmid- and protein-containing S. lividans TK24 grown on NMMP with 5 g/L casamino acids

To study the influence of plasmid maintenance and heterologous protein secretion on the metabolism, metabolic footprints are determined for the plasmid-containing strain (PL) and *S. lividans* TK24 producing mTNF-α (REC) and compared to the non-secreting wild type (WT). Figs. 2C–F and 6 depict growth, substrate utilization and metabolite accumulation in NMMP containing 5 g/L casamino acids of the PL and REC strains.

As for the wild type strain, two distinct growth phases are detected. The transition from GP1 to GP2 is triggered by (approximate) glutamate and aspartate depletion, and biomass growth eventually ceases due to glucose exhaustion. Opposed to the WT and PL strain growth profile, a clear adaptation period (without biomass growth) between GP1 and GP2 is identified for the protein-producing strain (see Figs. 2E, F and 6, dashed vertical line shows the end of the adaptation period). Values of the specific growth rates (Table 1) show the systematic decrease in specific growth rates for WT, PL and REC, respectively. Furthermore, the overall biomass yield decreases for WT, PL and REC, i.e., 4.81, 4.67 and 4.26 gDW/L, respectively. The reduced growth rate also influences the morphology as shown in Fig. 7. Microscopic images confirm that the slower growth coincides with the formation of bigger and denser clumps during the fermentations with the PL and REC.

The organic acid secretion profiles are significantly different for WT, PL and REC (see Fig. 2, right plots). Overall, the WT strain secretes more organic acids than the PL and REC strain, but other acids become predominant for PL and REC. PL and REC secrete much more lactate, the maximum concentration of which is higher for PL than for the REC strain. The PL and REC strain secrete a comparable amount of pyruvate, but this amount is much lower than produced by the WT strain. The highest levels of succinate and α-ketoglutarate are produced by the WT strain, while the PL strain produces almost no succinate and α-ketoglutarate.

Time profiles of the amino acid concentrations for PL and REC exhibit similar patterns, e.g., in terms of uptake sequence, as for the WT (compare Figs. 3 and 6, data PL not shown). Calculated yields and specific uptake rates, however, unveil some differences. Since the trend in the PL data, which behaves out of line with the WT and REC strain, is less clear, the focus is on the comparison of the REC and WT data.

The amount of alanine produced per gram biomass formed noticeably increases (Fig. 4), with its maximum attained at the start of GP2 (Fig. 6A). Fig. 4 shows that besides the increased assimilation of glucose and ammonium, the yield of most amino acids in GP1 increases, except for glutamate, aspartate, leucine and valine. In GP2, some amino acids are (nearly) depleted (e.g., serine, glutamate, aspartate) or are hardly consumed (e.g., valine, lysine, histidine). Note that some of these yields/specific rates are statistically not significantly different from zero although the data exhibit a decreasing trend. The yield of all other amino acids in GP2 is again higher in comparison to the WT strain and the yields of leucine and pro-

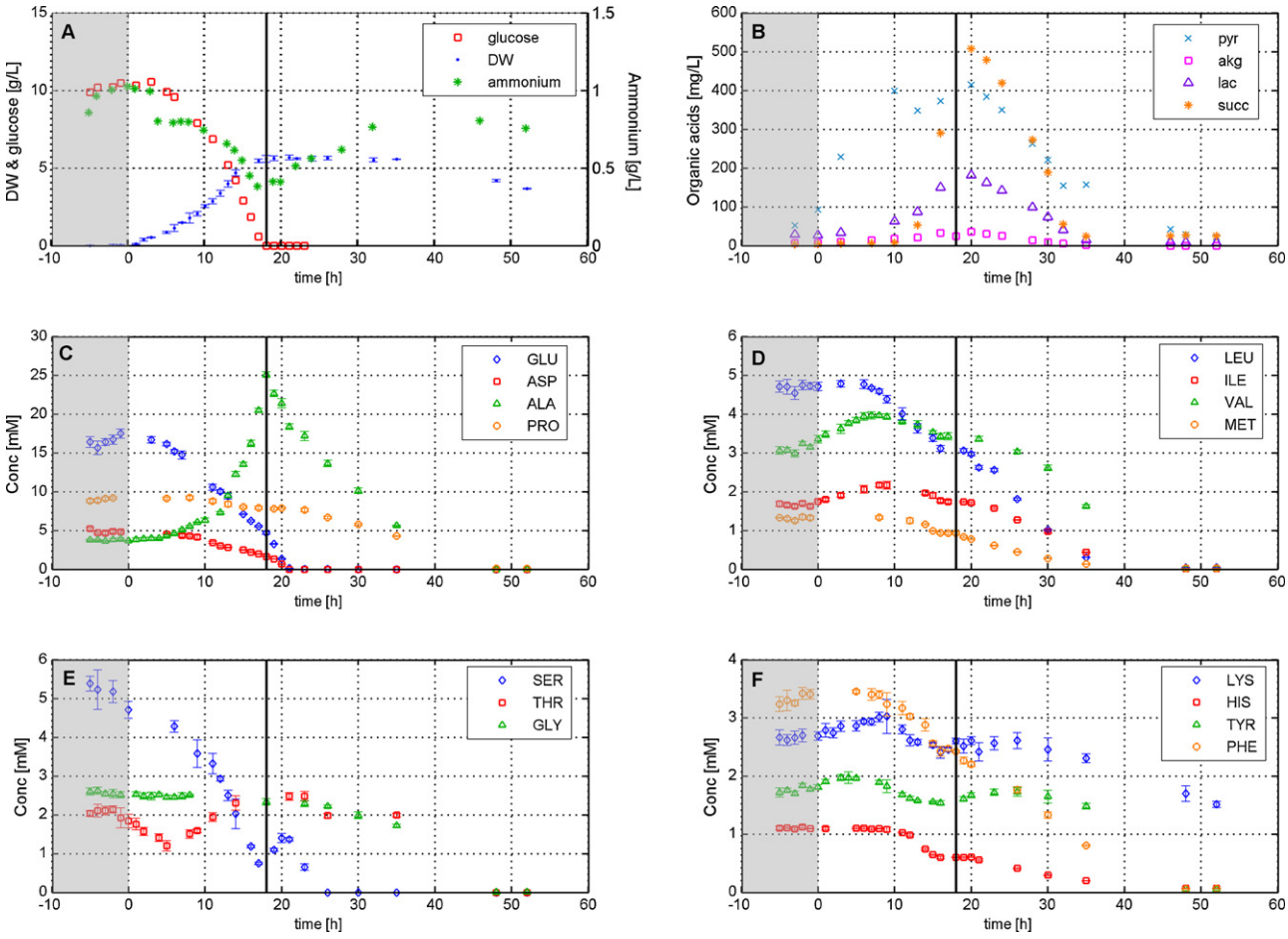

Fig. 5. Concentration profiles of *S. lividans* TK24 wild type strain (WT) grown on NMMP with 15 g/L casamino acids. (A) Biomass (●), glucose (□), ammonium (✱). (B) Pyruvate (×), Lactate (△), α-ketoglutarate (□), succinate (✱). (C) Glutamate (GLU), aspartate (ASP), alanine (ALA) and proline (PRO). (D) Leucine (LEU), isoleucine (ILE), valine (VAL) and methionine (MET). (E) Serine (SER), threonine (THR) and glycine (GLY). (F) Lysine (LYS), histidine (HIS), tyrosine (TYR) and phenylalanine (PHE). Vertical line demarcates the end of the growth phase (coinciding with glucose depletion).

line become most prominent. With respect to the WT strain, most specific uptake rates become smaller in GP1 but increase in GP2, whereas the specific glucose uptake rate is unchanged.

To conclude this section, the concentration profile of mTNF-α is presented in Fig. 8. Three production phases can be distinguished. Production is first observed in the first growth phase (GP1) at a rate of approximately 0.938 mg/gDW h. After transition to GP2 (with a lower growth rate), mTNF-α is produced at a significantly higher rate of 2.005 mg/gDW h until glucose is depleted. The protein yield of circa 80 mg/L at the end of the growth phase corresponds with the yield reported in Pozidis et al. (2001). During the stationary phase, a high production rate is maintained.

4. Discussion

4.1. Utilization of glutamate and aspartate for biomass growth

Comparison of the biomass profiles with the substrate concentration profiles revealed that the distinct growth phases (with different specific growth rates, see Table 1) coincide with the consumption of different substrates. In the first growth phase (GP1), glutamate and aspartate play a key role, because the depletion of these substrates determines the end of the first growth phase. In the second growth phase (GP2), characterized by a lower specific growth rate, glucose becomes the growth-limiting substrate, depletion of which determines the end of GP2.

Since the specific glucose uptake rate, as shown in Fig. 4, hardly differs between GP1 and GP2, the increased specific biomass growth rate in GP1 can most likely be attributed to glutamate and aspartate consumption. Utilization of glutamate and aspartate as both carbon and nitrogen sources by *Streptomyces* has previously been reported by, e.g., Williams and Katz (1977), Madden et al. (1996), Voelker and Altaba (2001) and Corvini et al. (2004). On the one hand, both amino acids, especially glutamate, play an important role in the central nitrogen metabolism (Hodgson, 2000). At high concentrations of ammonium, the glutamate dehydrogenase (GDH) transfers ammonium to glutamate which acts as the most important nitrogen donor in biosynthetic reactions. Glutamate also sequestrates ammonium through the glutamine synthetase/glutamate synthase (GS/GOGAT) system. The amine group of aspartate can be transferred to glutamate via an aspartate transaminase (AT). On the other hand, the carbon chain of glutamate and aspartate can enter the TCA cycle after deamination (by GDH and AT which yield α-ketoglutarate and oxaloacetate, respectively) and after catabolic breakdown (initiated by decarboxylation and eventually yielding succinate and acetyl-coA from glutamate and aspartate, respectively) (Hodgson, 2000; Borodina et al., 2005). Consequently, the latter part of the gluconeogenic pathway is most likely active and probably augments growth in GP1.

From the moment aspartate and glutamate are depleted, gamma-aminobutyric acid (GABA) is detected on the GC–MS chromatograms. GABA is formed by decarboxylation of glutamate

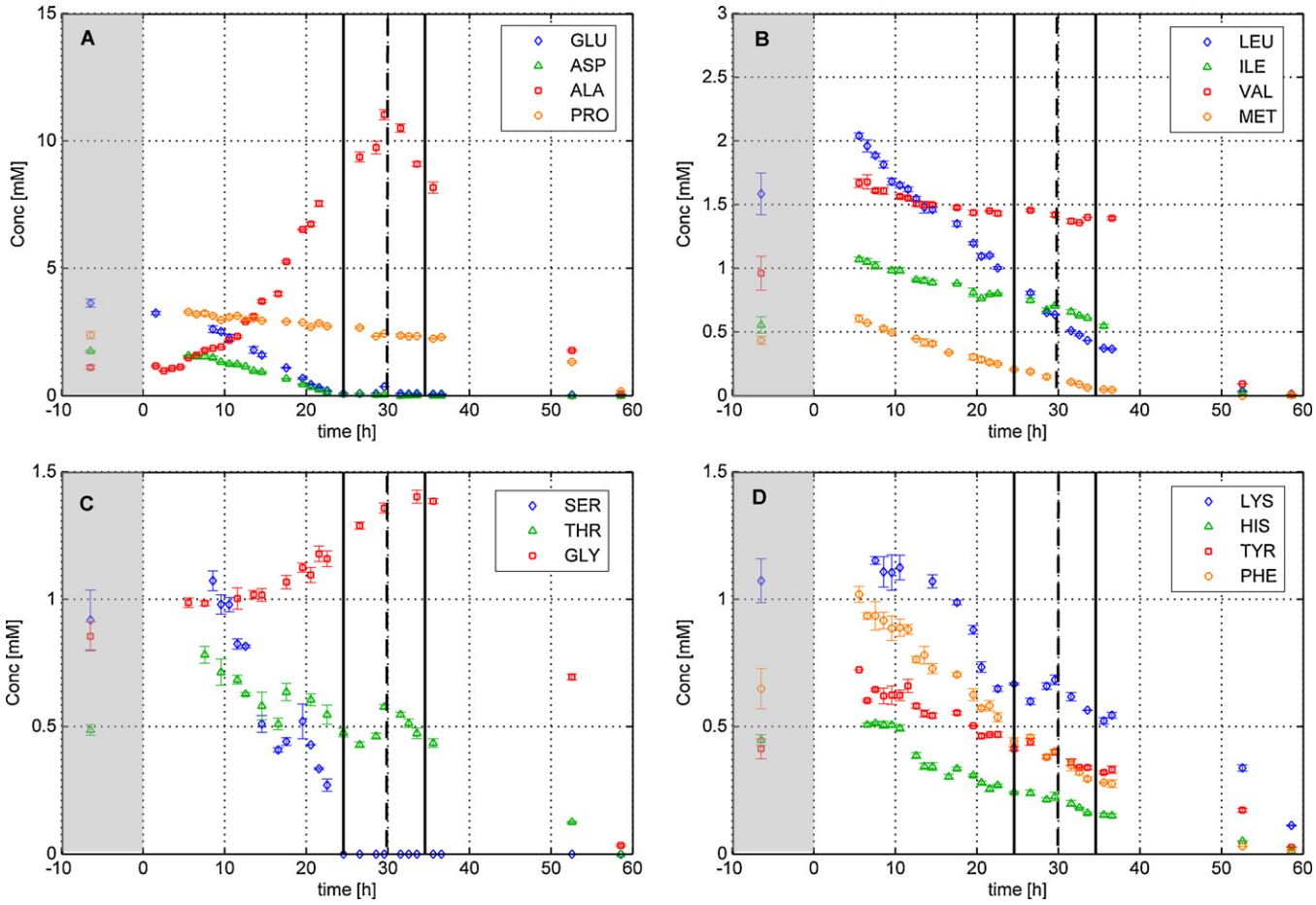

Fig. 6. Amino acid data for *S. lividans* TK24 protein-producing strain (REC) grown on NMMP containing 5 g/L casmino acids. (A) Glutamate (GLU), aspartate (ASP), alanine (ALA) and proline (PRO). (B) Leucine (LEU), isoleucine (ILE), valine (VAL) and methionine (MET). (C) Serine (SER), threonine (THR) and glycine (GLY). (D) Lysine (LYS), histidine (HIS), tyrosine (TYR) and phenylalanine (PHE). Full vertical lines demarcate growth phases (reflected by glutamate and aspartate depletion (GP1) and glucose depletion (GP2)). The dashed vertical line demarcates the end of the adaptation period (without growth) between GP1 and GP2 for the REC strain.

(Borodina et al., 2005). The secretion of GABA could thus reflect an adaptation of the intracellular pool in response to a metabolism shift from GP1 (with high fluxes in glutamate catabolism) to GP2 (in which biomass formation is mainly supported by glucose and ammonium).

Glutamate and aspartate usage and the associated increased growth rate, however, do not enhance heterologous protein secretion. Although using a constitutive promoter, no positive correlation between biomass growth rate and heterologous protein synthesis is observed (see further in Section 4.4).

4.2. Overflow metabolism during growth on NMMP supplemented with casamino acids

Excretion of organic acids as overflow metabolites in times of carbon excess is commonly observed in *Streptomyces* spp. (e.g., Madden et al., 1996; Karandikar et al., 1997; Avignone Rossa et al., 2002; Corvini et al., 2004; Colombié et al., 2005). Pyruvate and α-ketoglutarate are well known overflow metabolites, allowing cells to deal with this excess carbon resulting from a carbon flux bottleneck between the glycolysis and the TCA cycle (Hodgson, 2000, Colombié et al., 2005). For example, Madden et al. (1996) observed that *S. lividans* TK24 excretes pyruvate and α-ketoglutarate when glucose is the main carbon source, but they did not observe succinic acid or lactic acid production. In the present results, lactic acid accumulates during the entire growth phase. Although *Streptomycetes* are classified as strictly aerobic, their tendency to flocculate makes that the inside of the clumps grow probably micro-aerobically and produce lactate (Hockenhull et al., 1954; Borodina et al., 2005). Succinate production could also be caused by this oxygen limitation inside the kernels of the flocs but equally well may result from an imbalance of the carbon fluxes in the TCA cycle as shown by the WT experiment supplemented with 15 g/L casamino acids. Increasing the amount of amino acids results in more succinate production. Since only the amounts of amino acids is increased and thus, at least a part of, the succinate excretion is probably related with amino acids catabolism. During the stationary phase, when biomass accumulation ceases, all organic acids are taken up again.

Besides the organic acids, large amounts of alanine are detected in the medium. Taking in mind that GC–MS analysis can make no distinction between D- and L-alanine, the observed alanine production by *S. lividans* may be explained as follows. Firstly, part of the secretion can be related to the liberation of D-alanine in the peptidoglycan synthesis. Per gram of peptidoglycan formed 0.950 mmol of D-alanine is liberated outside the cell (values taken from Borodina et al., 2005). An estimate of the amount of D-alanine produced based on the amount of biomass formed and the typical amount of peptidoglycan per gram biomass explains only a very small fraction of the measured alanine concentration. Secondly, one may consider alanine excretion as an overflow phenomenon. Alanine is a very important amino acid for *Streptomyces*. Protein biosynthesis and peptidoglycan synthesis in *Streptomyces*, which are G+C rich bacteria, demand a lot of alanine (Borodina et al., 2005). The alanine synthesis flux will thus always be very high in

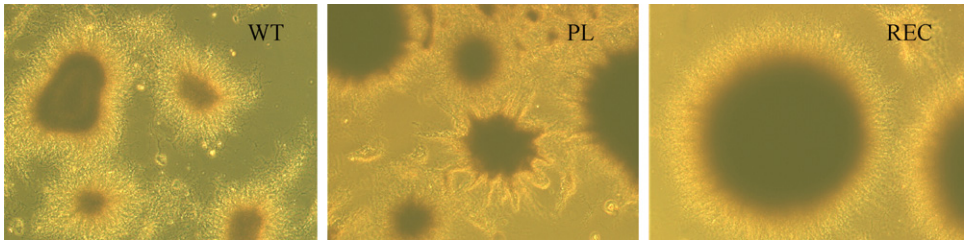

Fig. 7. Microscopic images for *S. lividans* TK24 wild type (WT), plasmid-containing (PL) and protein-producing (REC) strain taken near the end of biomass growth (end of GP2). Images were captured using a light microscope (Olympus BX 51) with phase contrast illumination (Ph1) and a total magnification of 100 times.

Streptomycetes. In most *Streptomycetes*, alanine is synthesized by the amination of pyruvate by the NAD-dependent alanine dehydrogenase (ADH).

The normal status for *Streptomycetes* in soil will be one of famine for nitrogenous compounds. In fermentation processes, however, that situation is often reversed by the addition of amino acids sources (like casamino acids). In the current experiments, amino acids are utilized simultaneously with glucose. Since biomass synthesis is slow (particularly in GP2), this may result in an excess of intracellular ammonium together with pyruvate overflow (see infra). ADH can then form alanine, hereby also reducing NADH into NAD^+. Consequently, (L-)alanine secretion may be assigned as an overflow metabolism dealing with the ammonium excess in the cell generated during amino acids catabolism (tripling the casamino acids content indeed increases alanine secretion), on the one hand, and the carbon excess in the cell generated during glucose catabolism. In this way, it helps to maintain the biochemical balance of the cell to assure the optimal operation of the metabolism under the governing circumstances. Given the importance of alanine in *Streptomyces*, ADH activity will anyway be high in *Streptomycetes* which strengthens this hypothesis. Similar as with the secreted organic acids, alanine is completely reused during the stationary phase.

Finally, glycine is considered. Uptake of this amino acid under the prevailing conditions is presumably inhibited by the presence of glucose in the medium (Hodgson, 2000) and thus there appears to be no uptake of glycine out of the medium during cell growth on glucose. Instead a small raise in the glycine concentration is noted (e.g., Figs. 3C and 6C), that should probably not been seen as an overflow but possibly arises from the lysis of death cells. The cell wall of *Streptomycetes* exists namely out of peptidoglycan which is very rich in glycine (Borodina et al., 2005).

4.3. Impact of heterologous protein production on the metabolic footprint

It is generally accepted that recombinant protein production places a metabolic burden on the host cell. Our experiments show that plasmid maintenance and heterologous protein overproduction elicit a noticeable change in *S. lividans* TK24, i.e., the biomass growth rate diminishes, bigger clumps are formed, substrates requirements change, and by-product accumulation alters (see Section 3.5).

Organic acids as well as alanine can be considered as unwanted by-products. The difference in the organic acid secretion pattern between WT, PL and REC can be explained in relation to morphology and recombinant protein synthesis. Part of the lactate formation by the REC strain can be assigned to the formation of bigger and denser clumps containing more cells inside the clumps experiencing a microaerobic environment (and thus secreting lactate). Heterologous protein production also requires more oxygen (Özkan et al., 2005). Comparing the dissolved oxygen levels at the end of GP2 (i.e., the lowest value reached) the dissolved oxygen percentage dropped to approximately 10% for the REC strain and 30% for the WT strain. The lower levels of pyruvate, α-ketoglutarate and succinate could be due to the fact that the fraction of actively growing cells (i.e., loose fragments and the periphery of the clumps) with respect to the total biomass has become smaller due to the dense floc formation and, consequently, the amounts of pyruvate, α-ketoglutarate and succinate decrease accordingly.

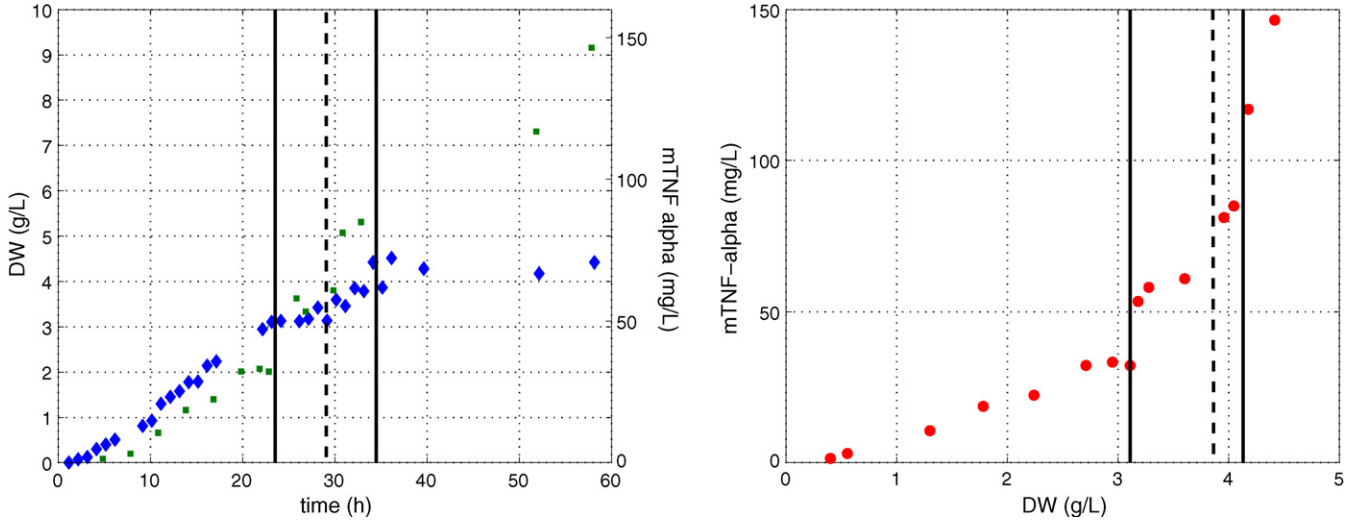

Fig. 8. mTNF-α concentration in relation to biomass formation. Left: mTNF-α concentration (■) and biomass concentration (♦) as a function of time during the batch experiment. Right: mTNF-α concentration with respect to the biomass concentration (●). Full vertical lines demarcate end of growth phases GP1 and GP2, the dashed vertical line demarcates the end of the adaptation period.

Alanine secretion increases for the REC in comparison to the WT strain (see Section 3.5). Alanine levels probably not only change outside the cell since Kassama et al. (2010) report an increased intracellular alanine concentration for *S. lividans* TK24 producing mTNF-α in phage medium which is also rich in amino acids. Given that alanine is thought to act as an overflow metabolite, the REC strain will experience a greater imbalance between catabolic and amphibolic pathways. In view of optimization of heterologous protein synthesis, overflow in terms of alanine and pyruvate should be minimized. Designing process control to maintain substrate levels preventing overflow, alanine and pyruvate monitoring can be used for process monitoring and as control input (Gerigk et al., 1998).

Although the demand for glucose and ammonium increased in the REC strain, the specific uptake rates for these substrates did not change. The increased requirement for glucose and ammonium can be assigned to the slow growth and protein synthesis (requiring energy, amino acids and reductive power). A somewhat unexpected observation is the lower specific uptake rates as well as lower yields for glutamate and aspartate. Unfortunately, no immediate explanation can be given to this result and the only way to understand this phenomenon is gaining deeper insight by, e.g., using techniques of metabolic flux analysis.

Yields of the other amino acids for REC compared to WT are altered and are particularly higher in GP2, which is also characterized by the highest protein synthesis. This shows the importance of the availability of amino acids for heterologous protein production. In GP2, yields of leucine and proline are highest. On the one hand, leucine (a branched chain amino acid) is known to contribute in protein synthesis, and thus possibly to heterologous protein synthesis. Leucine is also a prominent amino acid in mTNF-α. On the other hand, proline is a precursor for antibiotic production (see, Avignone Rossa et al., 2002) which is known to be formed but in this study not measured. Besides leucine, no clear link can be laid between the amino acid composition of mTNF-α and the uptake/requirements for particular amino acids. One possible way to identify which extracellular amino acids do affect mTNF-α secretion would for example be performing a sensitivity analysis based on a metabolic reaction network for the REC strain (testing the sensitivity of the amount of protein produced to changes in amino acid availability and type).

4.4. mTNF-α secretion in relation to biomass formation

Notwithstanding the increased carbon and nitrogen influx generated by glutamate and aspartate consumption, the yield of heterologous protein synthesis per gram dry weight and the specific protein secretion rate are lower in GP1 as in GP2 (Figure 8). In other words, glutamate and aspartate augment biomass growth but do not promote protein synthesis. The true cause behind this observation cannot be inferred from the current macroscopic data nor from available literature. This discrepancy between growth rate and protein yield is, however, important for process design. Tools for analysis of metabolic fluxes are required to pinpoint the correlation between substrate type, biomass growth rate and protein synthesis.

Interesting to note is that mTNF-α production slows down but does not stop during the stationary phase as long as *S. lividans* remains metabolically active (i.e., as long as organic acids and the remaining amino acids are consumed). This decoupling between cell growth and protein synthesis is often desirable in biotechnological applications (Weikert et al., 1998).

5. Conclusions

As illustrated in the present work, *S. lividans* grown on glucose, ammonium and a complex mixture of amino acids shows a complex overflow metabolism of organic acids and alanine. Whereas other microbial cell factories (like *E. coli*, *S. cerevisiae*, . . .) typically show carbon overflow which can easily be controlled by appropriate dosing of glucose, control of the carbon and nitrogen overflow in recombinant protein producing *S. lividans* requires more advanced control, both at the level of the carbon and nitrogen sources. Alternatively to advanced process control, metabolic engineering could be addressed to avoid overflow metabolism and maximize fluxes towards protein synthesis. Such an approach, however, requires more fundamental knowledge on the metabolic reaction network and the impact of environmental conditions on the flux distribution.

Besides the shift in the overflow metabolism, heterologous protein overproduction declines the biomass growth rate, correlates with extensive clump formation, and alters yield coefficients and specific conversion rates of amino acids. It is observed that *S. lividans* TK24 consumes glutamate and aspartate as preferential amino acids. In the absence of glutamate and aspartate, glucose and ammonium are the primary carbon and nitrogen resource but also amino acids are consumed. The strong preference of *Streptomycetes* for glutamate and aspartate is previously reported, but particularly interesting is that the present experiments indicate that the associated higher biomass formation rate reduces the heterologous protein yield. Intracellular resources generated by both substrates appear to be inefficiently or not directed into protein synthesis.

Current results do not yet provide a direct link between amino acid uptake and heterologous protein synthesis but indicate the importance of amino acids like glutamate, aspartate and leucine. Further investigation of the intracellular metabolic fluxes should be conducted to fully unravel the metabolic burden of plasmid maintenance and heterologous protein production and the importance of substrate choice and the control of substrate availability. In view of optimizing heterologous protein production, process design (selecting proper substrates and substrate(s) feeding) will be very important. From a more fundamental point of view, particular interest should go to the investigation of the central carbon and nitrogen metabolism and its regulation.

Acknowledgements

Work supported by the project FWO-G-08-00360 of the Research Foundation – Flanders (FWO), in part by projects OT/09/25 and EF/05/006 (OPTEC Optimization in Engineering) of the Research Council of the Katholieke Universiteit Leuven, by the Belgian Program on Interuniversity Poles of Attraction, initiated by the Belgian Federal Science Policy Office, and by FP6-EU Project no. LSHC-CT-2006-037834, and in the frame of ERA-IB project EIB.08.013. K. Bernaerts is a Postdoctoral Fellow with the Research Foundation – Flanders. J. Van Impe holds the chair Safety Engineering sponsored by the Belgian chemistry and life sciences federation essenscia. The authors thank Prof. B. Van der Bruggen (Department Chemical Engineering, KULeuven) for kindly providing access to GC–MS and PerkinElmer NV (Imperiastraat 8, 1930 Zaventem) for all GC-MS troubleshooting support. The scientific responsibility is assumed by its authors.

Appendix A. Supplementary data

Supplementary data associated with this article can be found, in the online version, at doi:10.1016/j.jbiotec.2010.08.011.

References

Avignone Rossa, C., White, J., Kuiper, A., Postma, P.W., Bibb, M., Teixeira de Mattos, M.J., 2002. Carbon flux distribution in antibiotic-producing chemostat cultures of *Streptomyces lividans*. Metab. Eng. 4, 138–150.

Ayadi, D.Z., Chouayekh, H., Mhiri, S., Zerria, K., Fathallah, D.M., Bejar, S., 2007. Expression by *Streptomyces lividans* of the rat α integrin CD11b A-domain as a secreted and soluble recombinant protein. J. Biomed. Biotechnol., 6, Article ID 54327.

Bapat, P.M., Das, D., Sohoni, S.V., Wangikar, P.P., 2006. Hierarchical amino acid utilization and its influence on fermentation dynamics: rifamycin B fermentation using *Amycolatopsis mediterranei* S699, a case study. Microb. Cell Fact. 5, 32.

Binnie, C., Cossar, J.D., Stewart, D.H.I., 1997. Heterologous biopharmaceutical protein expression in *Streptomyces*. Trends Biotechnol. 15, 315–320.

Borodina, I., Krabben, P., Nielsen, J., 2005. Genome-scale analysis of *Streptomyces coelicolor* A3(2) metabolism. Genome Res. 15, 820–829.

Colombié, V., Bideaux, C., Goma, G., Uribelarrea, J.L., 2005. Effects of glucose limitation on biomass and spiramycin production by *Streptomyces ambofaciens*. Bioproc. Biosyst. Eng. 28 (1), 1615–7591.

Corvini, P.F.X., Delaunay, S., Maujean, F., Rondags, E., Vivier, H., Goergen, J.-L., Germain, P., 2004. Intracellular pH of *Streptomyces pristinaespiralis* is correlated to the sequential use of carbon sources during the pristinamycins-producing process. Enzym. Microb. Technol. 34, 101–107.

Drummond, I.W., Shama, G., 1982. A rapid gas chromatographic method for the analysis of acidic fermentation products. Chromatographia 15 (3), 180–182.

Economou, A., 1999. Following the leader: bacterial protein export through the sec pathway. Trends Microbiol. 7, 315–320.

Gerigk, M., Bujnicki, R., Ganpo-Nkwenkwa, E., Bongaerts, J., Sprenger, G., Takors, R., 1998. Process control for enhanced L-phenylalanine production using different recombinant *Escherichia coli* strains. Biotechnol. Bioeng. 80 (7), 746–754.

Gilbert, M., Morosoli, R., Sharek, F., Kluepfel, D., 1995. Production and secretion of proteins by *Streptomycetes*. Crit. Rev. Biotechnol. 15 (1), 13–39.

Glick, B.R., 1995. Metabolic load and heterologous gene expression. Biotechnol. Adv. 13 (2), 247–261.

Görgens, J.F., van Zyl, W.H., Knoetze, J.H., Hahn-Hägerdal, B., 2005a. Amino acid supplementation improves heterologous protein production by *Saccharomyces cerevisiae* in defined medium. Appl. Microbiol. Biotechnol. 67, 684–691.

Görgens, J.H., Passoth, V., van Zyl, W.H., Knoetze, J.H., Hahn-Hägerdal, B., 2005b. Amino acid supplementation, controlled oxygen limitation and sequential double induction improves heterologous xylanase production by *Pichia stipitis*. FEMS Yeast Res. 5, 677–683.

Hockenhull, D.J., Fantes, K.H., Herbert, M., Whitehead, B., 1954. Glucose utilization by *Streptomyces griseus*. J. Gen. Microbiol. 10, 353–370.

Hodgson, D.A., 2000. Primary metabolism and its control in Streptomycetes: a most unusual group of bacteria. In: Pools, R.K. (Ed.), Advances in Microbial Physiology, vol. 42. Academic Press, pp. 47–238.

Karandikar, A., Sharples, G.P., Hobbs, G., 1997. Differentiation of *Streptomyces coelicolor* A3(2) under nitrate-limited conditions. Microbiology 143, 3581–3590.

Kassama, Y., Xu, Y., Dunn, W.B., Geukens, N., Anné, J., Goodacre, R., 2010. Assessment of adaptive focused acoustics versus manual vortex/freeze–thaw for intracellular metabolite extraction from *Streptomyces lividans* producing recombinant proteins using GC–MS and multi-block principal component analysis. Analyst, doi:10.1039/b918163f.

Kieser, T., Bib, M., Buttner, M., Chater, K., Hopwood, D., 2000. Practical Streptomyces Genetics. The John Innes Foundation.

Korn, F., Weingärtner, B., Kutzner, H.J., 1978. A study of twenty actinophages: morphology, serological relationship and host range. In: Freerksen, E., Tarnak, I., Thumin, J.H. (Eds.), Genetics of Actinomycetales. Fisher G, Stuttgart/New York, pp. 251–270.

Lammertyn, E., Van Mellaert, L., Schacht, S., Dillen, C., Sablon, E., Van Broekhoven, A., Anné, J., 1997. Evaluation of a novel subtilisin inhibitor gene and mutant derivatives for the expression and secretion of mouse tumor necrosis factor alpha by *Streptomyces lividans*. Appl. Environ. Microbiol. 63, 1808–1813.

Madden, T., Ward, J.M., Ison, A.P., 1996. Organic acid excretion by *Streptomyces lividans* TK24 during growth on defined carbon and nitrogen sources. Microbiology 142, 3181–3185.

Nakashima, N., Mitani, Y., Tamura, T., 2005. Actinomycetes as host cells for production of recombinant proteins. Microb. Cell Fact., 4–7.

Nowruzi, K., Elkamel, A., Scharer, J.M., Doug Cossar, D., Moo-Young, M., 2008. Development of a minimal defined medium for recombinant human interleukin-3 production by *Streptomyces lividans* 66. Biotechnol. Bioeng. 99, 214–222.

Özkan, P., Sariyar, B., Ütkür, F.O., Akman, U., Hortaçsu, A., 2005. Metabolic flux analysis of recombinant protein overproduction in *Escherichia coli*. Biochem. Eng. J. 22 (2), 167–195.

Pimienta, E., Ayala, J.C., Rodríguez, C., Ramos, A., Van Mellaert, L., Vallín, C., Anné, J., 2007. Recombinant production of *Streptococcus equisimilis* streptokinase by *Streptomyces lividans*. Microb. Cell Fact. 6, 20.

Pozidis, C., Lammertyn, E., Politou, A.S., Anné, J., Tsiftsologou, A.S., Sianidis, G., Economou, A., 2001. Protein secretion biotechnology using *Streptomyces lividans*: large-scale production of functional trimeric tumor necrosis factor alpha. Biotechnol. Bioeng. 72, 611–619.

Schaerlaekens, K., Lammertyn, E., Geukens, N., De Keersmaeker, S., Anné, J., Van Mellaert, L., 2004. Comparison of the Sec and Tat secretion pathways for heterologous protein production by *Streptomyces lividans*. J. Biotechnol. 112, 279–288.

Sianidis, G., Pozidis, C., Becker, F., Vrancken, K., Sjoeholm, C., Karamanou, S., Takano-Wik, M., Van Mellaert, L., Schaeffer, Th., Anné, J., Economou, A., 2006. Functional large-scale production of a novel *Jonesia sp.* xyloglucanase by heterologous secretion from *Streptomyces lividans*. J. Biotechnol. 121, 498–507.

Van Mellaert, L., Anné, J., 1999. Protein secretion in Gram-positive bacteria with high GC-content. Recent Res. Dev. Microbiol. 3, 425–440.

van Wely, K.H.M., Swaving, J., Freudl, R., Driessen, A.J.M., 2001. Translocation of proteins across the cell envelope of Gram-positive bacteria. FEMS Microbiol. Rev. 25, 437–454.

Voelker, F., Altaba, S., 2001. Nitrogen source governs the patterns of growth and pristinamycin production in *Streptomyces pristinaespiralis*. Microbiology 147, 2447–2459.

Vrancken, K., Anné, J., 2009. Secretory production of recombinant proteins by Streptomyces. Future Microbiol. 4 (2), 181–188.

Weikert, C., Sauer, U., Bailey, J., 1998. Increased phenylalanine production by growing and nongrowing *Escherichia coli* strain CWML2. Biotechnol. Prog. 14, 420–424.

Williams, W.K., Katz, E., 1977. Development of a chemically defined medium for the synthesis of Actinomycin D by *Streptomyces parvulus*. Antimicrob. Agents Chemother. 11 (2), 281–290.